Indian J. pure appl. Math., **28**(8) : 1133-1153, August 1997

REFLECTION AND TRANSMISSION OF ELASTIC WAVES AT A LOOSELY BONDED INTERFACE BETWEEN AN ELASTIC AND MICROPOLAR ELASTIC SOLID

RAJNEESH KUMAR AND BALJEET SINGH

Department of Mathematics, Kurukshetra University, Kurukshetra 136 119 *(Haryana)*

(*Received* 7 *February* 1996; *after revision* 24 *September* 1996; *accepted* 26 *December* 1996)

The problem of reflection and transmission of plane periodic waves incident on the loosely bonded interface between an elastic solid and a micropolar elastic solid is discussed with the assumption that the interface behaves like a dislocation which preserves the continuity of stress allowing a finite amount of slip. It is further assumed that the normal displacement is continuous and the shearing stress is proportional to the velocity of the slip. Amplitude ratios are computed numerically for a particular model and are plotted for different degree of bonding parameter. Two special cases have been discussed.

Key Words : Amplitude Ratios; Micropolar Elasticity; Slip; Bonding Parameter

INTRODUCTION

The linear theory of elasticity is of paramount importance in the stress analysis of steel, which is the commonest engineering structural material. To a lesser extent linear elasticity describes the mechanical behaviour of other common solid materials, e.g., concrete, wood and coal. However, the theory does not apply to the behaviour of many of the new synthetic materials of the elastomer and polymer type, e.g., polymethyl-methacrylate (perspex), polyethylene, polyvinyl chloride.

The micropolar theory of elasticity constructured by Eringen and his coworkers[1,2] and Palmov[12] intended to be applied on such materials and for such problems where the ordinary classical theory of elasticity fails because of microstructure in the material.

Metal, polymers, composites, solids, rocks, concrete are typical media with microstructures. Most of natural and manmade materials possess a microstructure. Classical elasticity is inadequate to represent the behaviour of such materials. The

discrepancy between the classical theory of elasticity and the experiments is particularly striking in dynamical problems, as in the case of elastic vibrations characterized by high frequency and small wave lengths, i.e., for ultrasonic waves. This discrepancy results from the fact that for high frequencies and small wave lengths, the influence of the body microstructure becomes significant. The classical theory of elasticity eventually fails in the case of vibrations of grain bodies and multimolecular bodies. The influence of the microstructure becomes here considerable, and result in development of new type of waves, not found in the classical theory of elasticity. When the wave length is of the same order of magnitude as the average dimension of the microelements, the intrinsic motions of the microelements with respect to the centre of mass of body can affect response appreciably. This situation prevails in practical applications when the material under consideration is a composite material containing macromolecules, fibres, and grains. Solid propellant grain, polymeric materials, and fibre glass are but a few examples of such materials.

A special micropolar material was fabricated in which uniformly distributed 'rigid' aluminium shot was cast in an elastic epoxy matrix. Gauthier[3] found this aluminium-epoxy composite to be micropolar material and investigated the values of the relevant parameters based on specimen of aluminium-epoxy composite.

Many problems of waves and vibrations have been discussed in micropolar elastic solids by several researchers. Notable among them are Parfitt and Eringen[4], Smith[5], Tomar and Gogna[6, 7], Tomar and Kumar[8], etc.

In problems of reflection and refraction of seismic waves at the interface between two elastic half-spaces, it is usually assumed that the half-spaces are in welded contact. However, the presence of liquid in the porous skeleton may weaken the welded contact at the interface. Hence it is reasonable to assume that a very thin layer of viscous liquid may be present at the interface and cause the two media to be loosely bonded. Murty[9] discussed a very interesting problem of reflection, transmission and attenuation of elastic waves at a loosely bonded interface between two elastic solid half-spaces by assuming that the interface behaves like a dislocation which preserves the continuity of traction allowing a finite amount of slip and derived the case of welded contact and ideally smooth interfaces as particular cases.

The micropolar theory of elasticity which was developed in sixties by Eringen and his coworkers[1, 2] and availability of experimental data for various parameters of the micropolar material provides us a chance to consider such problem of reflection and refraction where aluminium-epoxy composites as micropolar elastic solid is in loosely bonded contact with the crust as elastic solid. As such model may be found in the earth's crust, so the results of our problem can be applicable to the earth's crust, to a water-mud-rock boundary, or to some other specific problem in engineering or seismology like bedrock-soil interface or mantle-crust interface.

BASIC ASSUMPTIONS

Murty[9] defined a real parameter (bonding parameter) to which numerical values can be assigned corresponding to a given degree of bonding between half-spaces and discussed the cases of ideally smooth and fully bonded interfaces corresponding to

the values 0 and ∞ of the bonding parameter. Murty[9] carried his study by making two basic assumptions. The first assumption is that the loosely bonded interface between two solid half-spaces behaves as a Somigliana dislocation (Hill[10]) and assures continuity of traction across the interface. The second assumption is that there exists a complex linear relation between slip and local shear stress. Regarding the second assumption, Murty[9] suggested the only guiding principle that there must exist some relation between stress tensor and the 'slip' at the interface such that when shearing stress is zero, the 'slip' is undetermined and when the 'slip' vanishes the interface behaves as a welded contact. For numerical purpose, we may assume that

$$\text{Shearing stress} = K_s \times \text{slip} \qquad \ldots (1)$$

at the interface of loosely bonded media so that the vanishing of K_s corresponds to an ideally smooth interface, and infinitely large values of K_s correspond to a welded interface. The intermediate value of K_s represent a loosely bonded interface.

We assume a model of viscous layer between an elastic solid and micropolar elastic solid half-space. If the thickness of layer be D and η be the coefficient of viscosity. As $D \to 0$, the thickness of layer is infinitely small, therefore, it is appropriate to suppose the shearing stress at the interface in the following form

$$t_{zy} = \eta \left(\frac{\partial \dot{u}_2}{\partial z} \right), \qquad \ldots (2)$$

where $\dot{u}_2 = \dfrac{\partial u_2}{\partial t}$ and u_2 is the component of displacement along the interface and partial derivative is taken normal to the interface.

We can write eqn. (2) as

$$t_{zy} = \frac{\eta}{D} (\dot{u}_2 - \dot{u}'_2) \qquad \ldots (3)$$

where $\dot{u}_2 - \dot{u}'_2$ is the jump in the y-component of slip velocity across the layer. Assuming the pulse propagation to be time harmonic, equation (3) can be written as

$$t_{zy} = i\omega \left(\frac{\eta}{D} \right) (u_2 - u'_2) \qquad \ldots (4)$$

where ω is the angular frequency and the difference $u_2 - u'_2$ of displacement components parallel to the interface represents the slip.

BASIC EQUATIONS

Following Eringen[1], the equations of motion in a linear, isotropic, micropolar elastic medium without body and surface forces are given by

$$(C_1^2 + C_3^2)\, \nabla(\nabla \cdot \vec{u}) - (C_2^2 + C_3^2)\, \nabla \times (\nabla \times \vec{u}) + C_3^2\, \nabla \times \vec{\phi} = \ddot{\vec{u}}, \qquad \ldots (5)$$

$$(C_4^2 + C_5^2)\, \nabla(\nabla \cdot \vec{\phi}) - C_4^2\, \nabla \times (\nabla \times \vec{\phi}) + \omega_0^2\, \nabla \times \vec{u} - 2\omega_0^2 \vec{\phi} = \ddot{\vec{\phi}}, \qquad \ldots (6)$$

where

$$\left.\begin{aligned} C_1^2 &= (\lambda+2\mu)/\rho, & C_2^2 &= \frac{\mu}{\rho}, \\ C_3^2 &= \frac{K}{\rho}, & C_4^2 &= \frac{\gamma}{\rho J}, \\ C_5^2 &= \frac{(\alpha+\beta)}{\rho J}, & \omega_0^2 &= C_3^2/J = \frac{K}{\rho J}, \end{aligned}\right\} \quad \ldots (7)$$

$\lambda, \mu, K, \alpha, \beta, \gamma$ are material moduli, ρ is the density of the medium and J the microrotational inertia. $\vec{u}(\vec{x},t)$ and $\vec{\phi}(\vec{x},t)$ are displacement and microrotation vectors respectively.

Writing the vectors $\vec{u}$ and $\vec{\phi}$ as

$$\vec{u} = \nabla q + \nabla \times \vec{U}, \quad \nabla \cdot \vec{U} = 0, \quad \ldots (8)$$

$$\vec{\phi} = \nabla \xi + \nabla \times \vec{\psi}, \quad \nabla \cdot \vec{\psi} = 0. \quad \ldots (9)$$

Using the equations (8) and (9) in equations (5) and (6), we get

$$(C_1^2 + C_3^2)\ \nabla^2 q = \ddot{q}, \quad \ldots (10)$$

$$(C_4^2 + C_5^2)\ \nabla^2 \xi = 2\omega_0^2 \xi + \ddot{\xi}, \quad \ldots (11)$$

$$(C_2^2 + C_3^2)\ \nabla^2 \vec{U} + C_3^2\ \nabla \times \vec{\psi} = \ddot{\vec{U}}, \quad \ldots (12)$$

$$C_4^2\ \nabla^2 \vec{\psi} + \omega_0^2\ \nabla \times \vec{U} - 2\omega_0^2 \vec{\psi} = \ddot{\vec{\psi}}. \quad \ldots (13)$$

Parfitt and Eringen[4] have shown that there are four basic waves propagating with different phase velocities in an infinite micropolar elastic solid :

(i) A longitudinal displacement wave propagating with speed

$$V_1^2 = (\lambda + 2\mu + K)/\rho, \quad \ldots (14)$$

similar to that of dilatational wave of the classical theory of elasticity.

(ii) A longitudinal microrotational wave travelling with speed

$$V_2^2 = (\alpha+\beta+\gamma)/\left[\rho J\left(1 - \frac{2K}{\rho J \omega_c^2}\right)\right], \quad \ldots (15)$$

with its microrotation vector in the direction of propagation.

(iii) Two sets of coupled waves, one travelling with speed V_3 and the other with speed V_4 consist of transverse microrotation waves. V_3 and V_4 are given by

$$V_{3,4}^2 = \frac{1}{2(1-\chi)} [C_4^2 + C_3^2 + C_2^2 - (C_2^2 + C_3^2/2)\chi \pm \{C_4^2 - C_2^2 - C_3^2 + (C_2^2 + C_3^2/2)\chi]^2 + 2C_3^2 C_4^2 \chi\}^{1/2}], \quad \ldots (16)$$

where

$$\chi = 2\omega_0^2/\omega^2.$$

The waves travelling with velocities V_2 and V_3 can exist only when $\omega > \omega_c (= \sqrt{2}\,\omega_0)$; otherwise they degenerate into distance decaying vibrations from the source.

The force and couple stresses given by Eringen[1]

$$t'_{kl} = \lambda' u'_{r,r} \delta_{kl} + \mu' (u'_{k,l} + u'_{l,k}) + K' (u'_{l,k} - \varepsilon_{klr} \phi'_r), \quad \ldots (17)$$

$$m'_{kl} = \alpha' \phi'_{r,r} \delta_{kl} + \beta' \phi'_{k,l} + \gamma' \phi'_{l,k}, \quad \ldots (18)$$

where symbols have their usual meanings.

For a homogeneous isotropic elastic solid, the Helmholtz resolution for the displacement

$$u_e = \text{grad}\, \phi_e + \text{curl}\, \psi_e, \quad \ldots (19)$$

the potentials are found to satisfy the wave equation

$$\nabla^2 \phi_e = \frac{1}{\alpha^2} \frac{\partial^2 \phi_e}{\partial t^2}, \quad \ldots (20)$$

$$\nabla^2 \psi_e = \frac{1}{\beta^2} \frac{\partial^2 \psi_e}{\partial t^2}, \quad \ldots (21)$$

where

$$\alpha^2 = (\lambda_e + 2\mu_e)/\rho_e, \quad \beta^2 = \mu_e/\rho_e. \quad \ldots (22)$$

The stresses in classical elasticity is given by

$$t_{kl} = \lambda_e u_{r,r} \delta_{kl} + \mu_e (u_{k,l} + u_{l,k}). \quad \ldots (23)$$

Formulation of the Problem and its Solution

Let $M(Z > 0)$ and $M'(Z < 0)$ be the elastic and micropolar elastic half-spaces loosely bonded at a plane surface $Z = 0$. We assume that plane periodic waves (P or SV) are incident from the side which we designate as the region $Z > 0$. In this region,

we write all the variables without a prime, and we add a prime to denote the variables in the region $Z < 0$. The Z-axis is pointing downward into the medium M. The complete geometry of the problem is given in Fig. 1.

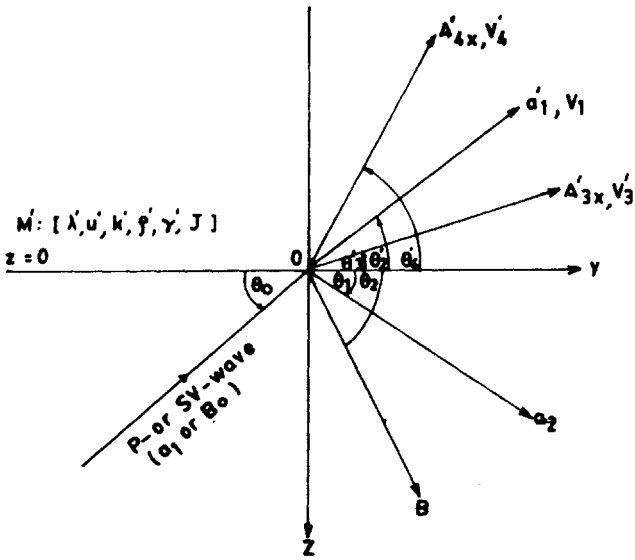

FIG. 1. Geometry of the problem.

The problem is two-dimensional in $(Y - Z)$ plane, therefore, we take

$$\vec{u} = (0, u_2, u_3), \qquad \ldots (24)$$

$$\vec{u'} = (0, u_2', u_3'), \quad \vec{\phi'} = (\phi_1', 0, 0), \qquad \ldots (25)$$

the components of displacement in elastic medium and the components of displacement and microrotation in micropolar elastic medium.

The appropriate potentials for this problem are given by :

In medium M : $(Z > 0)$

$$\phi_e = a_1 \exp[ik_1 (\cos\theta_0 y - \sin\theta_0 z) - i\omega_1 t] + a_2 \exp[ik_1 (\cos\theta_1 y + \sin\theta_1 z) - i\omega_1 t] \qquad \ldots (26)$$

$$\psi_e = B_0 \exp[ik_2 (\cos\theta_0 y - \sin\theta_0 z) - i\omega_2 t] + B \exp[ik_2 (\cos\theta_2 y + \sin\theta_2 z) - i\omega_2 t]. \qquad \ldots (27)$$

In medium M' : $(Z < 0)$

$$q' = a_1' \exp[ik_1' (\cos\theta_2' y - \sin\theta_2' z) - i\omega_1' t] \qquad \ldots (28)$$

$$\vec{U_p} = \hat{I}\ [A'_{px}] \exp\ [ik'_p\ (\cos\theta'_p\ y - \sin\theta'_p\ z) - i\omega'_p\ t] \qquad \ldots (29)$$

$$\vec{\Phi_p} = [B'_{py}\ \hat{J} + B'_{pz}\ \hat{K}\ ] \exp\ [ik'_p\ (\cos\theta'_p\ y - \sin\theta'_p\ z) - i\omega'_p\ t], \qquad \ldots (30)$$

where

$$\left.\begin{aligned} &\omega_i = k_i\ v_i, && (i = 1, 2)\ , \\ &\omega'_1 = k'_1\ v'_1\ , \\ &\omega'_p = k'_p\ v'_p\ , && (p = 3, 4)\ , \end{aligned}\right] \qquad \ldots (31)$$

a_1 (or B_0) and a_2, B are the amplitudes of incident P or (SV), and relfected P- and reflected SV-wave respectively; while a'_1 denotes the amplitude of refracted longitudinal displacement wave and $\vec{A'_p}$ and $\vec{B'_p}$ are the amplitudes of transverse displacement and transverse microrotational wave.

Parfitt and Eringen[4] derived the relation between the coefficients $\vec{A'_p}$ and $\vec{B'_p}$ as

$$\vec{B'_p} = -\left[\frac{i\,\omega'^2_0\,A'_{px}}{k'^2_p\,(v'^2_p - 2\omega'^2_0\,k'^{-2}_p - C'^2_p}\right](-\sin\theta'_p\,\hat{J} - \cos\theta'_p\,\hat{K}) \qquad \ldots (32)$$

BOUNDARY CONDITIONS

The boundary conditions at the loosely bonded interface $Z = 0$ between an elastic and a micropolar half-space are :

(i) Continuity of the normal force stress across the interface $Z = 0$, i.e.,

$$[t_{zz}]_M = [t'_{zz}]_{M'}\ .$$

(ii) Continuity of tangential force stress across the interface $Z = 0$, i.e.,

$$[t_{zy}]_M = [t'_{zy}]_{M'}.$$

(iii) Continuity of the normal displacement across the interface $Z = 0$, i.e.,

$$[u_3]_M = [u'_3]_{M'}\ .$$

(iv) The couple stress vanishes at $Z = 0$, i.e.,

$$0 = [m'_{zx}]_{M'}.$$

(v) Shearing force stress is proportional to the slip at the interface $Z = 0$. For numerical purpose, we shall write the last boundary condition as

$$[t_{zy}]_M = ik\mu_e \left(\frac{\zeta}{\cos\theta_0} \right)(u_2 - u_2'),$$

where

$$\zeta = \frac{\alpha\eta}{\mu_e D}, \text{ and } \theta_0 = \cos^{-1}\left(\frac{kV_0}{\omega} \right) \qquad \ldots (33)$$

is the angle of emergence and V_0 is the velocity of incident plane periodic wave.

It is convenient to introduce a variable ψ^*, $0 \le \psi^* \le 1$ such that $\zeta = \frac{\psi^*}{1-\psi^*}$.

The range $0 \le \zeta \le \infty$ shall be mapped on the range $0 \le \psi^* \le 1$. Thus $\psi^* = 0$ corresponds to a smooth surface and $\psi^* = 1$ corresponds to a welded interface between the two half-spaces. ψ^* may be considered as a bonding constant. Thus the last boundary condition can take the form

$$[t_{zy}]_M = ik\mu_e \frac{\psi^*}{(1-\psi^*)\cos\theta_0}(u_2 - u_2'). \qquad \ldots (34)$$

Substituting the values of potentials given by equations (26)-(30) in the above boundary conditions and making use of equations (8), (9), (17) - (19), (23) - (26), (32) and (34), the Snell's law given by

$$\frac{\cos\theta_0}{V_0} = \frac{\cos\theta_1}{\alpha} = \frac{\cos\theta_2}{\beta} = \frac{\cos\theta_1'}{V_1'} = \frac{\cos\theta_3'}{V_3'} = \frac{\cos\theta_4'}{V_4'} \qquad \ldots (35)$$

where

$$V_0 = \begin{cases} \alpha & \text{for an incident P–wave} \\ \beta & \text{for an incident SV–wave} \end{cases} \qquad \ldots (36)$$

and assuming

$$\omega_1 = \omega_2 = \omega_1' = \omega_3' = \omega_4' = \omega \text{ (say) at } Z = 0. \qquad \ldots (37)$$

We obtain a set of five non-homogeneous equations and these equations can be written in compact form as

$$\sum_{j=1}^{5} a_{ij} Z_j = b_i, \qquad (i = 1, 2, \ldots, 5), \qquad \ldots (38)$$

where Zj, (j = 1, 2, ..., 5) are the amplitude ratios of reflected P-, reflected SV-, refracted longitudinal displacement, coupled transverse displacement and coupled transverse microrotational waves, respectively, and

$$a_{11} = \left[\frac{\lambda_e}{K'} + \frac{2\mu_e}{K'} \left\{ 1 - \left(\frac{\alpha}{V_0} \right)^2 \cos^2 \theta_0 \right\} \right] \left(\frac{V_0}{\alpha} \right)^2,$$

$$a_{12} = \frac{2\mu_e}{K'} \cos \theta_0 \frac{V_0}{\beta} \sqrt{1 - \left(\frac{\beta}{V_0} \right)^2 \cos^2 \theta_0}$$

$$a_{13} = -\left[\frac{\lambda'}{K'} + D_1 \left\{ 1 - \left(\frac{V_1'}{V_0} \right)^2 \cos^2 \theta_0 \right\} \right] \left(\frac{V_0}{V_1'} \right)^2$$

$$a_{14} = -D_1 \cos \theta_0 \frac{V_0}{V_3'} \sqrt{1 - (V_3'/V_0)^2 \cos^2 \theta_0}$$

$$a_{15} = -D_1 \cos \theta_0 \frac{V_0}{V_4'} \sqrt{1 - (V_4'/V_0)^2 \cos^2 \theta_0}$$

$$a_{21} = -\frac{2\mu_e}{K'} \cos \theta_0 \frac{V_0}{\alpha} \sqrt{1 - \left(\frac{\alpha}{V_0} \right)^2 \cos^2 \theta_0}$$

$$a_{22} = \frac{\mu_e}{K'} \left(\frac{V_0}{\beta} \right)^2 \left[2 \left(\frac{\beta}{V_0} \right)^2 \cos^2 \theta_0 - 1 \right]$$

$$a_{23} = -D_1 \frac{V_0}{V_1'} \cos \theta_0 \sqrt{1 - (V_1'/V_0)^2 \cos^2 \theta_0}$$

$$a_{24} = -\left(\frac{V_0}{V_3'} \right)^2 \left[\frac{\mu'}{K'} \left\{ 2 \left(\frac{V_3'}{V_0} \right)^2 \cos^2 \theta_0 - 1 \right\} - \sqrt{1 - (V_3'/V_0)^2 \cos^2 \theta_0} - \frac{1}{R_1'} \right]$$

$$a_{25} = -\left(\frac{V_0}{V_4'} \right)^2 \left[\frac{\mu'}{K'} \left\{ 2 \left(\frac{V_4'}{V_0} \right)^2 \cos^2 \theta_0 - 1 \right\} - \sqrt{1 - (V_4'/V_0)^2 \cos^2 \theta_0} - \frac{1}{R_2'} \right]$$

$$a_{31} = \frac{V_0}{\alpha} \sqrt{1 - \left(\frac{\alpha}{V_0} \right)^2 \cos^2 \theta_0}$$

$$a_{32} = -\cos \theta_0, \quad a_{33} = \frac{V_0}{V_1'} \sqrt{1 - (V_1'/V_0)^2 \cos^2 \theta_0}$$

$$a_{34} = \cos \theta_0, \quad a_{35} = \cos \theta_0, \quad a_{41} = a_{42} = a_{43} = 0$$

$$a_{44} = \frac{1}{R_1'} \sqrt{1 - (V_3'/V_0)^2 \cos^2 \theta_0}$$

$$a_{45} = \frac{1}{R_1'} \sqrt{1 - (V_4'/V_0)^2 \cos^2 \theta_0} \Big/ \left(\frac{V_4'}{V_3'} \right)^3$$

$$a_{51} = \cos \theta_0 \left[\psi^* - 2(1 - \psi^*) \frac{\alpha}{V_0} \sqrt{1 - \left(\frac{\alpha}{V_0} \right)^2 \cos^2 \theta_0} \right]$$

$$a_{52} = \left(\frac{V_0}{\beta} \right)^2 \left[\left\{ 2 \left(\frac{\beta}{V_0} \right)^2 \cos^2 \theta_0 - 1 \right\} (1 - \psi^*) + \psi^* \frac{\beta}{V_0} \sqrt{1 - \left(\frac{\beta}{V_0} \right)^2 \cos^2 \theta_0} \right]$$

$$a_{53} = - \psi^* \frac{\alpha}{V_0} \cos \theta_0$$

$$a_{54} = \psi^* \frac{\alpha}{V_3'} \sqrt{1 - (V_3'/V_0)^2 \cos^2 \theta_0}$$

$$a_{55} = \psi^* \frac{\alpha}{V_4'} \sqrt{1 - (V_4'/V_0)^2 \cos^2 \theta_0}$$

and

b_i (i = 1, 2, ..., 5) will be as :

(a) For an incident P-wave

$$b_1 = - a_{11}, \; b_2 = a_{21}, \; b_3 = a_{31}, \; b_4 = 0,$$

$$b_5 = - \cos \theta_0 [\psi^* + 2(1 - \psi^*) \sin \theta_0]$$

(b) For an incident SV-wave

$$b_1 = a_{12}, \; b_2 = - a_{22}, \; b_3 = a_{32}, \; b_4 = 0,$$

$$b_5 = - [\cos 2\theta_0 (1 - \psi^*) - \psi^* \sin \theta_0]$$

where

$$D_1 = \frac{2\mu'}{K'} + 1, \; R_1' = \frac{\omega^2}{\omega_0'^2} - 2 - \frac{C_4'^2 k_3'^2}{\omega_0'^2},$$

$$R_2' = \frac{\omega^2}{\omega_0'^2} - 2 - \frac{C_4'^2 k_4'^2}{\omega_0'^2}.$$

SPECIAL CASES

(A) To discuss the problem of reflection and refraction of plane harmonic waves at an interface between the elastic solid and micropolar elastic solid half-space in welded contact, we put $\psi^* = 1$ in the boundary conditions and obtain a set of five non-homogeneous equations which can be written in compact form as :

$$\sum_{j=1}^{5} a_{ij}^* Z_j = b_i^*, \quad (i = 1, 2, ..., 5) \qquad \text{... (39)}$$

where

$$a_{ij}^* = a_{ij} \quad (i, j = 1, 2, 3, 4)$$

$$a_{51}^* = \cos\theta_0$$

$$a_{52}^* = \frac{V_0}{\beta}\sqrt{1-\left(\frac{\beta}{V_0}\right)^2 \cos^2\theta_0}$$

$$a_{53}^* = -\frac{\alpha}{V_0}\cos\theta_0$$

$$a_{54}^* = \frac{\alpha}{V_3'}\sqrt{1-(V_3'/V_0)^2\cos^2\theta_0}$$

$$a_{55}^* = \frac{\alpha}{V_4'}\sqrt{1-(V_4'/V_0)^2\cos^2\theta_0}$$

$$b_i^* = b_i \quad (i = 1, 2, ..., 4)$$

$$b_5^* = \begin{cases} -a_{51}^* & \text{for incident P–wave} \\ a_{52}^* & \text{for incident SV–wave.} \end{cases}$$

(B) If we let $K' = \gamma' = 0$ and replace θ_0 by $\theta_0 - 90^\circ$ in the system of equations (38), we obtain a set of four non-homogeneous equations, which again can be written in compact form as

$$\sum_{j=1}^{4} C_{ij} Z_j^* = d_i, \quad (i = 1, 2, ..., 4) \qquad \text{... (40)}$$

where

$$C_{11}=\left[\lambda_e+2\mu_e\left\{1-\left(\frac{\alpha}{V_0}\right)^2\sin^2\theta_0\right\}\right]\left(\frac{V_0}{\alpha}\right)^2$$

$$C_{12}=2\mu_e\sin\theta_0\frac{V_0}{\beta}\sqrt{1-\left(\frac{\beta}{V_0}\right)^2\sin^2\theta_0}$$

$$C_{13}=-\left[\lambda'+2\mu'\left\{1-\left(\frac{V_1'}{V_0}\right)^2\sin^2\theta_0\right\}\right]\left(\frac{V_0}{V_1'}\right)^2$$

$$C_{14}=-2\mu'\sin\theta_0\frac{V_0}{V_3}\sqrt{1-(V_3'/V_0)^2\sin^2\theta_0}$$

$$C_{21}=-2\mu_e\sin\theta_0\frac{V_0}{\alpha}\sqrt{1-\left(\frac{\alpha}{V_0}\right)^2\sin^2\theta_0}$$

$$C_{22}=\mu_e\left(\frac{V_0}{\beta}\right)^2\left\{2\left(\frac{\beta}{V_0}\right)^2\sin^2\theta_0-1\right\}$$

$$C_{23}=-2\mu'\frac{V_0}{V_1'}\sin\theta_0\sqrt{1-(V_1'/V_0)^2\sin^2\theta_0}$$

$$C_{24}=-\mu'\left(\frac{V_0}{V_3'}\right)^2\left\{2\left(\frac{V_3'}{V_0}\right)^2\sin^2\theta_0-1\right\}$$

$$C_{31}=\frac{V_0}{\alpha}\sqrt{1-\left(\frac{\alpha}{V_0}\right)^2\sin^2\theta_0}$$

$$C_{32}=-\sin\theta_0,\quad C_{33}=\frac{V_0}{V_1'}\sqrt{1-(V_1'/V_0)^2\sin^2\theta_0}$$

$$C_{34}=\sin\theta_0$$

$$C_{41}=\sin\theta_0\left[\psi^*-2(1-\psi^*)\frac{\alpha}{V_0}\sqrt{1-\left(\frac{\alpha}{V_0}\right)^2\sin^2\theta_0}\right]$$

$$C_{42}=\left(\frac{V_0}{\beta}\right)^2\left[\left\{2\left(\frac{\beta}{V_0}\right)^2\sin^2\theta_0-1\right\}(1-\psi^*)+\psi^*\frac{\beta}{V_0}\sqrt{1-\left(\frac{\beta}{V_0}\right)^2\sin^2\theta_0}\right]$$

$$C_{43} = -\psi^* \frac{\alpha}{V_0} \sin\theta_0$$

$$C_{44} = \psi^* \frac{\alpha}{V_3'} \sqrt{1 - (V_3'/V_0)^2 \sin^2\theta_0}$$

and

d_i, $(i = 1, 2, ..., 4)$ will be as :

(a) For an incident P-wave

$$d_1 = -C_{11},\ d_2 = C_{21},\ d_3 = C_{31},\ d_4 = -\sin\theta_0 [\psi^* + 2(1 - \psi^*)\cos\theta_0].$$

(b) For an incident SV-wave

$$d_1 = C_{12},\ d_2 = -C_{22},\ d_3 = C_{32},\ d_4 = \cos 2\theta_0 (1 - \psi^*) + \psi^* \cos\theta_0.$$

with the constraints $K' = \gamma' = 0$, we observe that

$$V_1'^2 = (\lambda' + 2\mu')/\rho' = \alpha' \qquad \ldots (41)$$

the speed of longtitudinal wave in elastic medium

$$V_3'^2 = \mu'/\rho' = \beta', \qquad \ldots (42)$$

the speed of shear wave in the elastic medium and $V_4' = 0$, implying that the corresponding coupled transverse microrotational wave does not exist and hence $A_{4x}' = 0$.

If we let $V_0 = \alpha$ in eqn. (40), then these equations correspond to the case of incident P-wave at a loosely bonded interface discussed by Murty[9].

NUMERICAL RESULTS

Following Bullen[11], we have the following values of density and elastic parameter for crust as elastic solid

$$\lambda_e = 2.238 \times 10^{11} \text{ dyne/cm}^2$$

$$\mu_e = 2.992 \times 10^{11} \text{ dyne/cm}^2$$

$$\rho_e = 2.65 \text{ gm/cm}^3.$$

Following Gauther[3], we have the following values of density and micropolar elastic parameters for aluminium epoxy composite as micropolar elastic solid

$$\lambda' = 7.59 \times 10^{11} \text{ dyne/cm}^2, \qquad \rho' = 2.19 \text{ gm/cm}^3$$

$$\mu' = 1.89 \times 10^{11} \text{ dyne/cm}^2, \qquad J' = 0.196 \text{ cm}^2$$

$$K' = 0.0149 \times 10^{11} \text{ dyne/cm}^2, \qquad \omega^2/\omega_0^2 = 10.$$

A computer programme has been developed and amplitude ratios of various reflected and refracted waves have been computed. For the frequency ratio ω^2/a_0^2 = 10, the variation of these amplitude ratios with the angle of emergence have been shown in Figs. 2 to 25.

(i) Incident P-Wave

The variations of amplitude ratios with the angle of emergence of the incident P-wave have been studied for the values of bonding constant ψ^* = 0.0, 0.25, 0.50, 0.75, 1.00. The nature of dependence of amplitude ratios of different reflected and refracted waves on the angle of emergence is, however, different for different values of the bonding constant. The variations of amplitude ratios $|Z_i|$, (i = 1, 2, ..., 5) with the angle of emergence for different values of bonding constant are shown in Figs. 2 to 14.

It is observed that the amplitude ratios $|Z_1|$ of reflected P-waves for different values of bonding constants have some initial value one at $\theta_0 = 0°$. For $\psi^* = 0.0$ and $\psi^* = 0.25$, it decreases sharply to values $0.2e - 001$ and $0.514e - 002$ at $\theta_0 = 8°$ respectively. Beyond $\theta_0 = 8°$, it increases to values 0.3843 and 0.378 at $\theta_0 = 34°$ for $\psi^* = 0.0$ and $\psi^* = 0.25$ respectively, thereafter, it decreases uniformly for both the values of bonding constant. For $\psi^* = 0.50$, the amplitude ratio of reflected P-wave decreases sharply to a value $2.279e - 002$ at $\theta_0 = 6°$. For the range $6° \leq \theta_0 \leq 28°$, it also increases and attains a value 0.393 at $\theta_0 = 28°$. Beyond $\theta_0 = 28°$, it decreases uniformly. The variations of amplitude ratios of reflected P-wave for $\psi^* = 0.75$ and $\psi^* = 1.0$ is different from the amplitude ratios of reflected P-wave for $\psi^* = 0.0$, 0.25, 0.50. For $\psi^* = 0.75$ and $\psi^* = 1.0$, the reflected P-wave has oscillating character. For $\psi^* = 0.75$ the amplitude ratio of reflected P-wave oscillates for the range $0° \leq \theta_0 \leq 90°$, attaining two peaks, one at $\theta_0 = 26°$ and the other at $\theta_0 = 55°$, while for $\psi^* = 1.0$ it has its maxima at $\theta_0 = 34°$, though oscillates. These variations have been shown in Figs. 2, 12, 13 and 14 respectively.

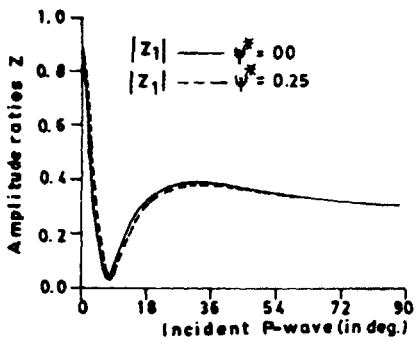

FIG. 2

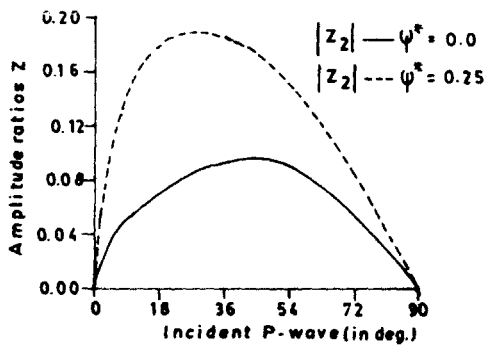

FIG. 3

The amplitude ratio $|Z_2|$ of the reflected SV-wave with the angle of emergence is different for different values of bonding constant. It obtained the value zero at

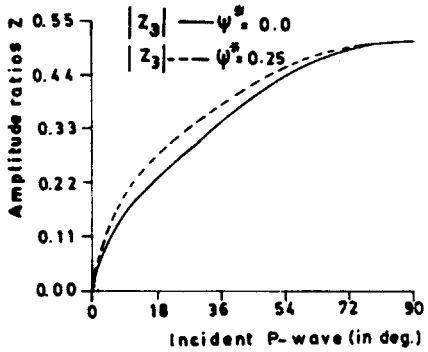

FIG. 4

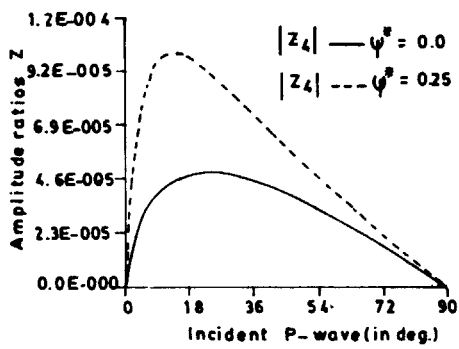

FIG. 5

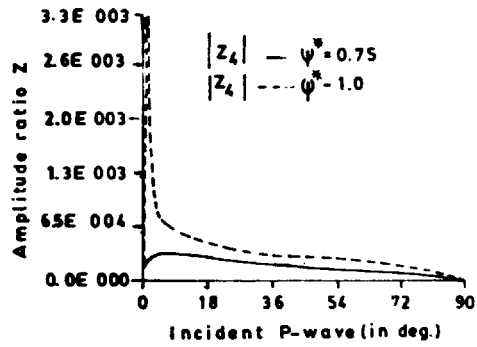

FIG. 6

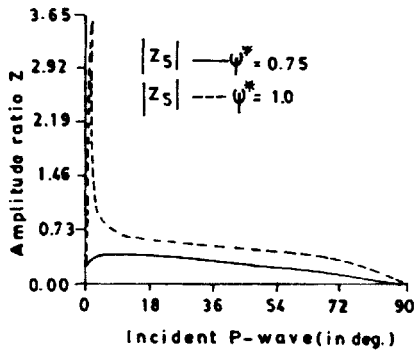

FIG. 7

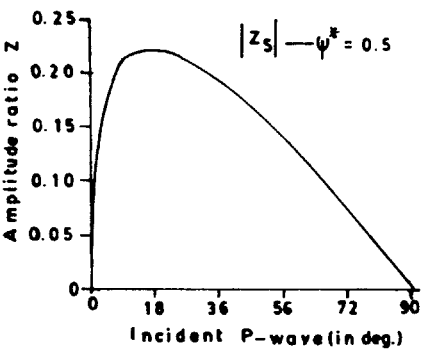

FIG. 8

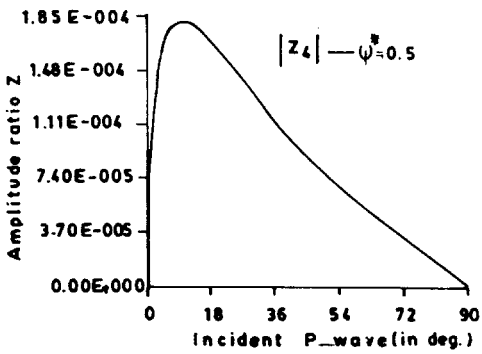

FIG. 9

$\theta_0 = 0°$ for $\psi^* = 0.0, 0.25, 0.50, 0.75, 1.00$. For $\psi^* = 0.0, 0.25, 0.50$, the amplitude ratio $|Z_2|$ first increases and then decreases as θ_0 varies from 0° to 90°. It attains its maxima at $\theta_0 = 43°, 29°, 18°$ for $\psi^* = 0.0, 0.25, 0.50$ respectively. The amplitude ratios of relfected SV-wave for $\psi^* = 0.75$ and $\psi^* = 1.0$ are different from those for $\psi^* = 0.0, 0.25, 0.50$. For $\psi^* = 0.75$, it increases sharply to a very high value at

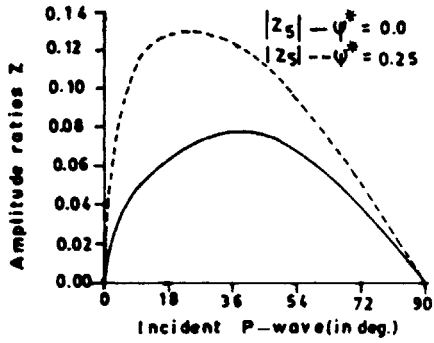

FIG. 10

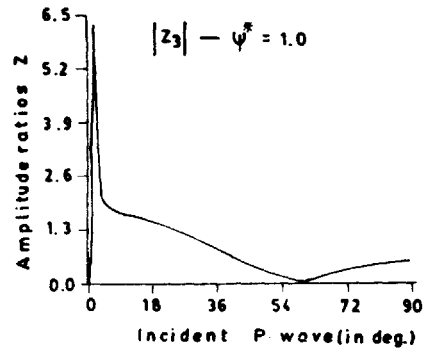

FIG. 11

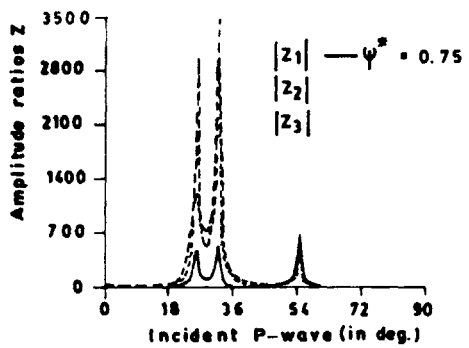

FIG. 12

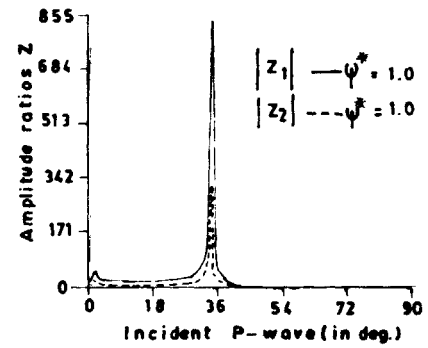

FIG. 13

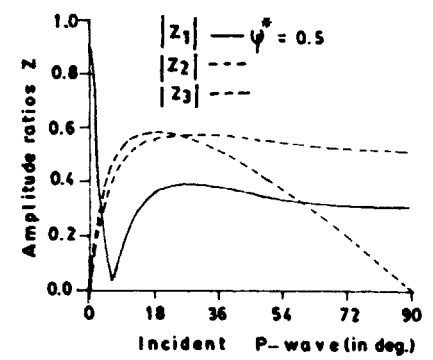

FIG. 14

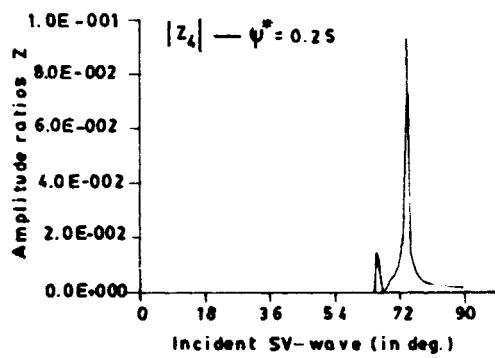

FIG. 15

$\theta_0 = 26°$ and oscillates for the range $26° \leq \theta_0 \leq 36°$, getting its maxima at $\theta_0 = 34°$. Beyond 34°, ° it decreases sharply to zero at $\theta_0 = 90°$. For $\psi^* = 1.0$, it oscillates for the range $0° \leq \theta_0 \leq 34°$, attaining its maxima at $\theta_0 = 34°$, thereafter, it decreases. These variations have been shown in Figs. 3, 12, 13 and 14 respectively.

The amplitude ratio $|Z_3|$ of refracted longitudinal displacement wave has its

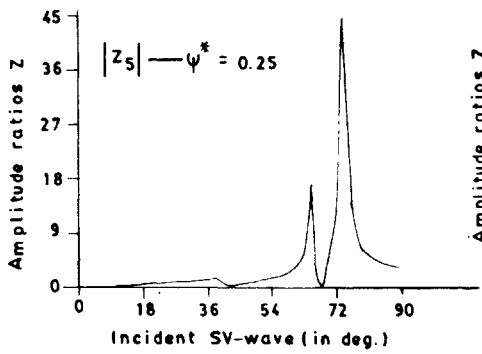

FIG. 16

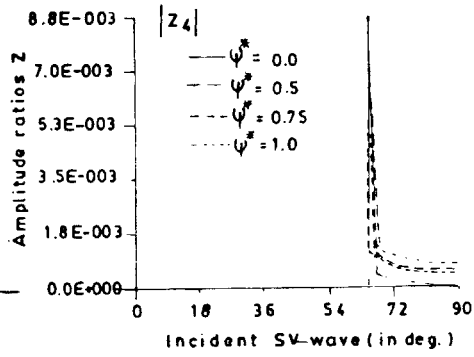

FIG. 17

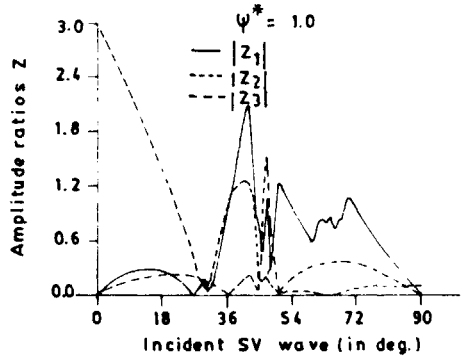

FIG. 18

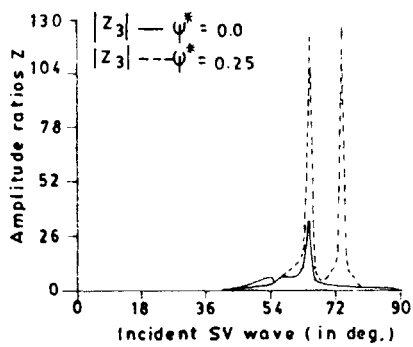

FIG. 19

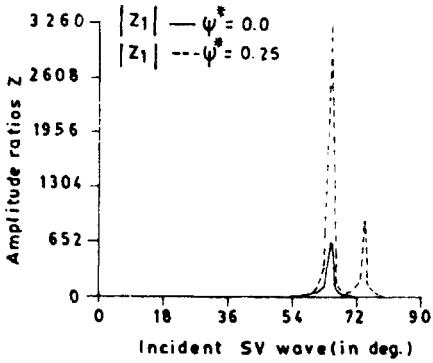

FIG. 20

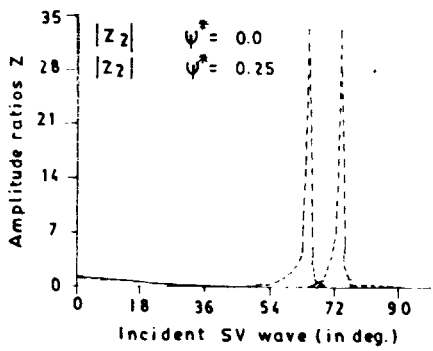

FIG. 21

value zero at $\theta_0 = 0°$ for $\psi^* = 0.0, 0.25, 0.50, 0.75, 1.00$. For $\psi^* = 0.0$ and 0.25, it increases slowly to the value 0.5101 at $\theta_0 = 90°$. For $\psi^* = 0.50$, it increases sharply to value 0.5747 at $\theta_0 = 28°$, thereafter, it decreases uniformly to 0.5101 at $\theta_0 = 90°$. For $\psi^* = 0.75$ and $\psi^* = 1.0$, the variation of amplitude ratios of the refracted longitudinal displacement wave is different from those for $\psi^* = 0.0, 0.25,$

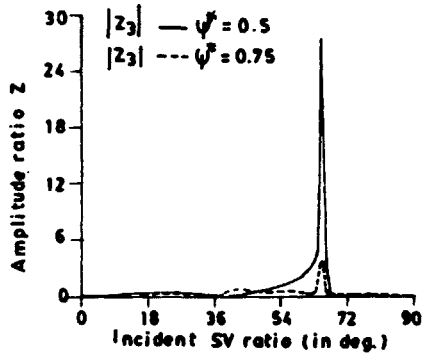

FIG. 22

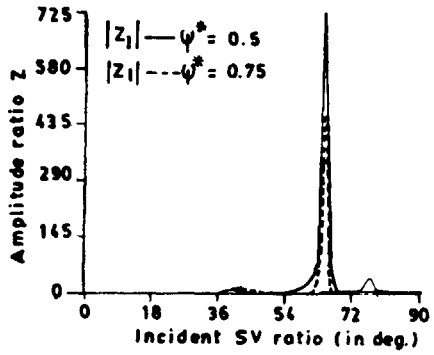

FIG. 23

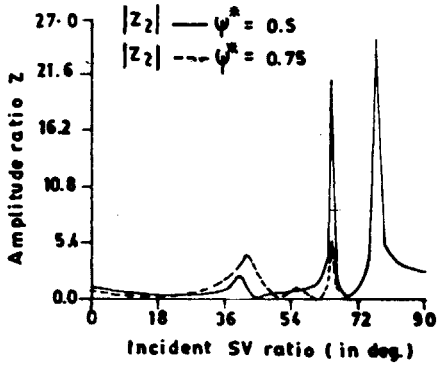

FIG. 24

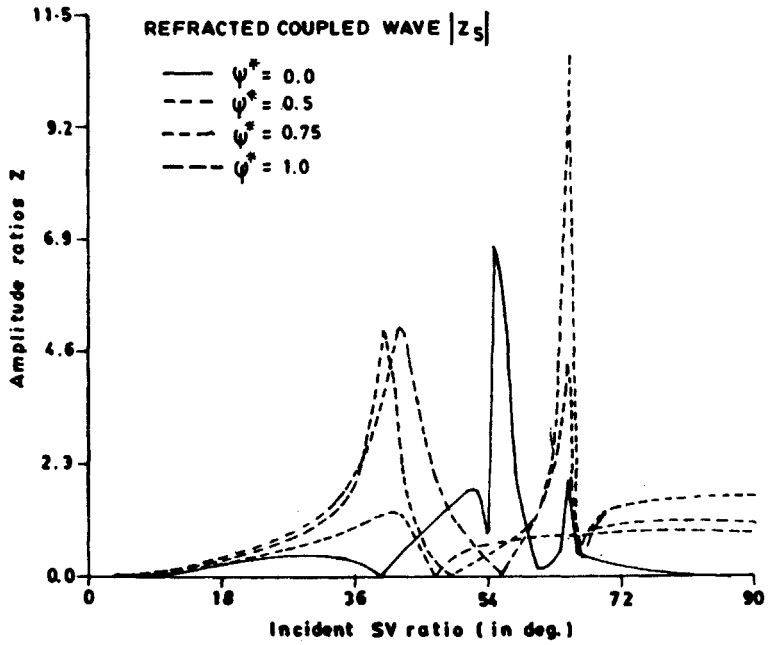

FIG. 25

0.50. For $\psi^* = 0.75$, it increases sharply attaining two peaks at $\theta_0 = 26°$ and $\theta_0 = 32°$. Beyond $\theta_0 = 32°$, it decreases to a value 1.147e – 002 at $\theta_0 = 77°$ and increases again to a value 0.5101 at $\theta_0 = 90°$. For $\psi^* = 1.0$, it increases to a value 6.346 at $\theta_0 = 2°$ and decreases uniformly to a value 1.138e – 002 at $\theta_0 = 60°$. It again increases to a values 0.5101 at $\theta_0 = 90°$. It is observed that the refracted longitudinal displacement wave is not affected by looseness of boundary when $\theta_0 = 0°$ and $\theta_0 = 90°$. These variations have been depicted in Figs. 4, 11, 12 and 14 respectively.

The amplitude ratios $|Z_4|$ and $|Z_5|$ of refracted coupled waves have similar variations with the angle of emergence for different values of bonding constants. Both the waves start with zero amplitude at $\theta_0 = 0°$ for $\psi^* = 0.0, 0.25, 0.50, 0.75, 1.00$. The amplitude ratios of these refracted coupled waves first increases and then decreases to a value nearly zero as θ_0 varies from 0° to 90° for different values of bonding constant. The variations of the amplitude ratios $|Z_4|$ and $|Z_5|$ of refracted coupled waves have been depicted in Figs. 5 to 10. These diagram clearly shows the effect of looseness on set of refracted coupled waves.

It may be concluded that the amount of slip increases with the angle of emergence and approaches to a maximum in the range 25° to 35°. However, when the incidence is very near grazing incidence, the effect of interface becomes immaterial as expected.

(ii) Incident SV-Wave

Likewise in case of an incident P-wave, an incident SV-wave gives rise to reflected P-, SV, refracted longitudinal displacement and a set of two refracted coupled waves. The manner in which the amplitude ratios of different reflected and refracted waves vary with the angle of emergence is different for different values of ψ^*. These variations have been shown in Figs. 15 to 25.

The amplitude ratio $|Z_1|$ of reflected P has its value zero at $\theta_0 = 0°$ for $\psi^* = 0.0, 0.25, 0.50, 0.75, 1.00$. For $\psi^* = 0.0$, the amplitude ratio $|Z_1|$ first increases sharply attaining its maxima at $\theta_0 = 65°$ and decreases sharply a value nearly zero at $\theta_0 = 90°$. For $\psi = 0.25$ and 0.75 the amplitude ratio $|Z_1|$ oscillates as θ_0 varies from 0° to 45°. Beyond $\theta_0 = 45°$, it increases sharply to its maxima at $\theta_0 = 65°$ and decreases sharply to value near zero at $\theta_0 = 90°$. For $\psi^* = 0.5$ it oscillates as θ_0 varies from 0° to 90° attaining sharp maxima at $\theta_0 = 65°$. In case of welded interface, it also oscillates as θ_0 varies from 0° to 90° and attains three peak values at $\theta_0 = 42°, 50°, 70°$ respectively. These variations have been depicted in Figs. 20, 23 and 18 respectively.

The amplitude ratio $|Z_2|$ of reflected SV-wave has its value one at $\theta_0 = 0°$ for $\psi^* = 0.0, 0.25, 0.50, 0.75, 1.00$. For $\psi^* = 0.0$, it decreases to a value nearly zero at $\theta_0 = 45°$, thereafter, it oscillates and finally attains its value one at $\theta_0 = 90°$. For $\psi^* = 0.25$, it decreases slowly to its value 2.317e-002 at $\theta_0 = 42°$, thereafter, it increases sharply to its maxima at $\theta_0 = 65°$. As θ_0 varies, it first decreases sharply

and again increases sharply to a value near maximum value at $\theta_0 = 74°$. Beyond $\theta_0 = 74°$, it first decreases sharply and then oscillates minutely. For $\psi^* = 0.50$ it decreases uniformly to value 0.384 at $\theta_0 = 25°$. For the range $25° \leq \theta_0 \leq 90°$, it oscillates getting its peak values at $\theta_0 = 65°$ and $\theta_0 = 77°$ respectively. For $\psi^* = 0.75$, it decreases sharply to a value 0.1677 at $\theta_0 = 16°$. Beyond $\theta_0 = 16°$, it oscillates getting its peak values at $\theta_0 = 42°$, 56° and 65° respectively. In case of welded interface, it has its maximum value 2.923 at $\theta_0 = 1°$. For the range $1° \leq \theta_0 \leq 90°$, it oscillates. These variations have been shown in Figs. 21, 24 and 18 respectively.

The amplitude ratio $|Z_3|$ of refracted longitudinal displacement wave has its value zero at $\theta_0 = 0°$. For $\psi^* = 0.0$, it oscillates minutely as θ_0 varies from 0° to 58°. Beyond $\theta_0 = 58°$, it increases sharply attaining its maxima at $\theta_0 = 65°$ and decreases sharply to a value nearly zero at $\theta_0 = 90°$. For $\psi^* = 0.25$, it oscillates as θ_0 varies from 0° to 90° having its peak values at $\theta_0 = 65°$ and $\theta_0 = 74°$. For $\psi^* = 0.5$, it also oscillates as θ_0 varies from 0° to 90° and attains its maxima at $\theta_0 = 65°$. For $\psi^* = 0.75$, it oscillates as θ_0 varies from 0° to 90° having its peak values at $\theta_0 = 20°$, 42° and $\theta_0 = 65°$. In case of welded contact, it has similar variation as that for $\psi^* = 0.75$, with the exception that it attains its peak values at $\theta_0 = 20°$, 42° and 69°. These variations have been shown in Figs. 19, 22 and 18 respectively.

The amplitude ratio $|Z_4|$ of refracted coupled wave remains zero as θ_0 varies from 0° to 65° for all values of bonding constant ψ^*. In case of smooth interface, it has its value 3.805*e*-003 at $\theta_0 = 66°$. It decreases sharply to a value nearly zero at $\theta_0 = 90°$. For $\psi^* = 0.25$ and 0.50, it has its values 1.516*e*-002 and 8.736*e*-003 respectively at $\theta_0 = 66°$. For these values of bonding constant, it first oscillates and then decreases slowly as θ_0 varies from 0° to 90°. For $\psi^* = 0.75$ and 1.00, it has its values 2.02*e*-003 and 7.159*e*-003 respectively at $\theta_0 = 66°$. Beyond $\theta_0 = 66°$, it decreases uniformly for $\psi^* = 0.75$ and 1.00. These variations have been shown graphically in Figs. 15 and 17.

The amplitude ratio $|Z_5|$ of the another refracted coupled wave has its value zero at $\theta_0 = 0°$ for all values of bonding constant ψ^*. For the case of smooth interface, it increases slowly to a value 0.4558 at $\theta_0 = 31°$. Beyond $\theta_0 = 31°$, it oscillates attaining its peak values at $\theta_0 = 52°$, 55° and 65° and finally decreases to a value nearly zero at $\theta_0 = 90°$. For $\psi^* = 0.25$, it increases slowly to a value 1.358 at $\theta_0 = 37°$. As θ_0 varies from 37° to 42°, it decreases sharply and then increases sharply to value 17.51 at $\theta_0 = 65°$. As θ_0 varies from 65° to 68°, it decreases sharply and then increases very sharply attaining its maxima at $\theta_0 = 74°$. As $\theta_0 \geq 74°$, it decreases sharply to a value 3.049 at $\theta_0 = 90°$. For $\psi^* = 0.5$, it increases slowly to value 5.136 at $\theta_0 = 40°$. As θ_0 varies from 40° to 67°, it oscillates getting its maxima at $\theta_0 = 65°$. Beyond $\theta_0 = 67°$, it increases very slowly to a value 1.652 at $\theta_0 = 90°$. For $\psi^* = 0.75$, it increases slowly to its maximum value 5.149 at $\theta_0 = 42°$ and then decreases to a value 6.162*e*-002 at $\theta_0 = 56°$. It again increases sharply to a value 4.497 at $\theta_0 = 65°$ and decreases very sharply to a value 2.377*e*-001 at $\theta_0 =$

66°. As θ_0 varies from 67° to 90°, it increases slowly to a value 1.091 at $\theta_0 = 90°$. In case of welded interface, it increases slowly to its maximum value 1.391 at $\theta_0 = 42°$ and then decreases sharply to a value 3.488*e*-002 at $\theta_0 = 47°$. Beyond $\theta_0 = 47°$, it increases slowly getting its value 0.9342 at $\theta_0 = 80°$. As θ_0 varies from 80° to 90°, it decreases minutely. These variations have been shown in Figs. 16 and 25.

It may be concluded that in case of incident SV-wave, the amount of slip is maximum in the range 60° to 70° and the effect of loosely bonded interface becomes immaterial when the incidence is very near to grazing incidence.

CONCLUSION

Numerical calculations in detail have been presented for the case of both P- and SV-waves incident at the interface of model considered and the results obtained agree fairly with those of Murty[6] For all values ψ' discussed in the problem, it is observed that amplitude ratio changes with the change of bonding parameter ψ' and the rate of change of the amplitude ratio is not uniform. It is also observed that for the both cases of striking waves, most of the energy gets reflected and the energy transmitted across the interface is maximum along the refracted longitudinal displacement wave and energy transported by a set of two refracted coupled waves is very small. Therefore, the assumption of loosely bonded interface instead of welded will affect the reflection-refraction phenomenon considerably. It may represent a more realistic form of the earth model and may be of the interest for experimental seismologist.

ACKNOWLEDGEMENT

One of the authors Baljeet Singh is highly thankful to the C.S.I.R., New Delhi for its kind financial support in this research work.

REFERENCES

1. A. C. Eringen, *Theory of Micropolar Elasticity, Fracture*, Vol. 2, Academic Press, New York, 1968.
2. A. C. Eringen and E. S. Suhubi, *Int. J. Engng. Sci* 2(2) (1964) 189; 2(4) (1964) 389.
3. R. D. Gauthier, *Experimental Investigations on Micropolar Media, p. 395, Mechanics of Micropolar Media* (ed.: O. Brulin and R.K.T. Hsieh), World Scientific Singapore 1982.
4. V. R. Parfitt and A. C. Eringen, *J. Acoust. Soc. Am.* 45 (1969), 1258-69.
5. A. C. Smith, *Int. J. Engng. Sci.* 10 (5) (1967), 741.
6. S. K. Tomar and M. L. Gogna, *Int. J. Engng. Sci.* 30 (1992), 1637-46.
7. S. K. Tomar and M. L. Gogna, *Int. J. Engng. Sci.* 33(1995), 485-496.
8. S. K. Tomar and R. Kumar, *Int. J. Engng. Sci.* 33 (1995), 1507-1515.
9. G. S. Murty, *Geophys. J. R. astron. Soc.* 44 (1976), 389-404.
10. R. Hill, *Progress in Solid State Mechanics*, Vol. II, Chapter 6, p. 268 (eds.: I.N. Sneddon and R. Hill) North Holland Publishing, Amsterdam, Netherlands, 1961.
11. K. E. Bullen, *An Introduction to Theory of Seismology*, Cambridge University Press, Cambridge, 1963.
12. N. A. Palmov, *Prikl. Mat. Mekh.* 28 (1964), 401.